Society For Biomaterials

Fabrication, characterization, and biocompatibility assessment of a novel elastomeric nanofibrous scaffold: A potential scaffold for soft tissue engineering

Elham Shamirzaei Jeshvaghani,[1] Laleh Ghasemi-Mobarakeh,[1] Reza Mansurnezhad,[1] Fatemeh Ajalloueian,[2] Mahshid Kharaziha,[3] Mohammad Dinari,[4] Maryam Sami Jokandan,[2] Ioannis S. Chronakis[2]

[1]Department of Textile Engineering, Isfahan University of Technology, Isfahan, 8415683111, Iran
[2]Research Group for Nano-Bio Science, National Food Institute, Technical University of Denmark, Kgs. Lyngby, Denmark
[3]Department of Materials Engineering, Isfahan University of Technology, Isfahan, 8415683111, Iran
[4]Department of Chemistry, Isfahan University of Technology, Isfahan, 8415683111, Iran

Received 20 April 2017; revised 15 September 2017; accepted 16 October 2017
Published online 00 Month 2017 in Wiley Online Library (wileyonlinelibrary.com). DOI: 10.1002/jbm.b.34043

Abstract: With regard to flexibility and strength properties requirements of soft biological tissue, elastomeric materials could be more beneficial in soft tissue engineering applications. The present work investigates the use of an elastic polymer, (polycaprolactone fumarate [PCLF]), for fabricating an electrospun scaffold. PCLF with number-average molecular weight of 13,284 g/mol was synthetized, electrospun PCLF:polycaprolactone (PCL) (70:30) nanofibrous scaffolds were fabricated and a novel strategy (*in situ* photocrosslinking along with wet electrospinning) was applied for crosslinking of PCLF in the structure of PCLF:PCL nanofibers was presented. Sol fraction results, Fourier-transform infrared spectroscopy, and mechanical tests confirmed occurrence of crosslinking reaction. Strain at break and Young's modulus of crosslinked PCLF:PCL nanofibers fabricated was found to be $114.5 \pm 3.9\%$ and 0.6 ± 0.1 MPa, respectively, and dynamic mechanical analysis results revealed elasticity of nanofibers. MTS assay showed biocompatibility of PCLF:PCL (70:30) nanofibrous scaffolds. Our overall results showed that electrospun PCLF:PCL nanofibrous scaffold could be considered as a candidate for further *in vitro* and *in vivo* experiments and its application for engineering of soft tissues subjected to *in vivo* cyclic mechanical stresses. © 2017 Wiley Periodicals, Inc. J Biomed Mater Res Part B: Appl Biomater 00B: 000–000, 2017.

Key Words: polycaprolactone fumarate, polycaprolactone, electrospinning, elastomer, soft tissue engineering

How to cite this article: Shamirzaei Jeshvaghani, E, Ghasemi-Mobarakeh, L, Mansurnezhad, R, Ajalloueian, F, Kharaziha, M, Dinari, M, Sami Jokandan, M, Chronakis, IS 2017. Fabrication, characterization, and biocompatibility assessment of a novel elastomeric nanofibrous scaffold: A potential scaffold for soft tissue engineering. J Biomed Mater Res Part B 2017:00B:000–000.

INTRODUCTION

Soft tissue plays connecting, supporting and protecting roles for organs and also has an aesthetic role in natural body shape.[1,2] Contour irregularity and defects of soft tissue are increasing due to both acquired and congenital reasons such as traumatic injury, infection, and extirpation. It is thus clear that harms of these defects on physical and emotional well-being of patients has caused a large demand for soft tissue regeneration strategies.[1–5] Transplantation of autologous tissue and prostheses are the general treatment for soft tissue regeneration. However, these two approaches have their own limitations. Autologous implantation suffers from absorption of autologous tissues and donor shortage while lack of some requirements such as permanence and shortage in fully accomplish of all organ function are reasons of artificial prostheses failure.[2,4,6]

Considering that many soft tissues that are subject to cyclic mechanical stresses *in vivo*, such as cardiovascular tissues and blood vessels have elastomeric properties,[6–11] low moduli biopolymers with an elastic nature, such as elastomers which are either physically or chemically crosslinked, would be preferable for soft tissue engineering applications. However, it is often difficult to fully match the mechanical properties of target tissue. Among different biopolymers, elastomers show high extensibility and recover to their original state when removing the stress. They are made of long polymer chains with excellent degree of flexibility and mobility.[6,12]

Correspondence to: L. Ghasemi-Mobarakeh; e-mail: laleh.ghasemi@cc.iut.ac.ir
Contract grant sponsor: Danish Research Council Foundations; contract grant number: DFF-4093-00282 and 4217-00048A
Contract grant sponsor: Denmark and Iran (Isfahan University of Technology-isfahan-Iran)

Polyester elastomers prepared by polycondensation of polyols and multifunctional carboxylic acids have attracted much interest for tissue engineering applications. Polycaprolactone fumarate (PCLF) has been developed as a crosslinkable and unsaturated fumarate-based derivative of polycaprolactone (PCL). It is biocompatible and due to representing broad range of mechanical properties, has been used as a promising material for nerve and bone tissue engineering.[13–16]

Nanofibrous scaffolds are one of the scaffold types which have been used for soft tissue engineering applications. Such scaffolds benefit from high surface area to volume ratio and dimensional similarity with native extracellular matrix, making them an interesting substrate for tissue engineering applications.[17–22] Based on the importance of nanofibrous elastomeric scaffolds in soft tissue regeneration, this study aimed to synthesize PCLF and fabricate it to PCLF nanofibrous scaffolds. Due to the lack of spinnability of PCLF, PCL was further blended with PCLF in different ratios and PCLF:PCL nanofibrous scaffolds were fabricated by electrospinning. In the previous studies, PCLF scaffolds were produced in the form of film by casting of PCLF solution, followed by irradiation of solution under ultraviolet (UV) light and drying.[16,23,24] To the best of our knowledge, there is no report on crosslinking of PCLF in the solid state and fabricating PCLF in the form of nanofibers.

In this study, we used different methods for crosslinking of PCLF in order to achieve a scaffold with elastomeric properties. *In vitro* cell culture study was also performed to investigate the biocampatibilty of nanofibrous scaffolds.

MATERIALS AND METHODS

Materials

PCL diol (Mw = 2000 g/mol), PCL (Mw = 70,000–90,000 g/mol), and bis-acylphosphinoxide (BAPO) as UV photoinitiator were purchased from Sigma-Aldrich (St. Louis, MO). Fumaryl chloride (FuCl), calcium hydride (CaH_2) as drying agent, potassium carbonate (K_2CO_3) as proton scavenger, dichloromethane (CH_2Cl_2), *N*,*N*-dimethylmethanamide (DMF) and acetic acid (CH_3COOH) as solvents were all obtained from Merck Company (Germany). N2 gas (99.99%) and phosphate buffered saline (PBS) were purchased from Ardestan Gas Co. (Ardestan, Iran) and Bioidea Company (Iran), respectively. Dulbecco's modified Eagle medium (DMEM) was purchased from Gibco. Fetal bovine serum, penicillin, and streptomycin were obtained from Sigma-Aldrich (Denmark). Cell Titer 96 AQueous Non-Radioactive Cell Proliferation Assay 3-(4,5-dimethylthiazol-2-yl)-5-(3-carboxymethoxyphenyl)-2-(4-sulfophenyl)-2H-tetrazolium (MTS) was purchased from Promega, Madison, WI.

Synthesis and characterization of PCLF

Polymer synthesis. Polymerization was performed in a 250 mL three-necked reaction flask fitted with a reflux condenser and purged with N_2 and equipped with raw material entrance. Prior to copolymerization, a certain amount of PCL diol was dried overnight in a vacuum oven at 50°C for 48 h to remove any residual water. FuCl was purified by distillation at 161°C under vacuum and dichloromethane was dried and distilled over CaH_2 before the reaction. FuCl, PCL diol, and K_2CO_3 were measured out in a molar ratio of 1:1:1.2, respectively. First, K_2CO_3 was added to a three-neck flask and then PCL diol in dichloromethane was added to K_2CO_3 and stirred to form slurry. FuCl dissolved in CH_2Cl_2 was added dropwise to the reaction vessel under reflux for 12 h. After the completion of polymerization, the reaction mixture was cooled down and transferred to centrifuge tubes and spun down for 15 min at 4000 rpm to remove unreacted K_2CO_3 completely. The supernatant was precipitated into petroleum ether and then solvent was removed by rotary evaporator. The polymer was dried in a vacuum oven at room temperature for at least 12 h and stored at −20°C until used.

Characterization of synthesized PCLF. Chemical analysis of the synthesized PCLF was performed by Fourier-transform infrared spectroscopy (FTIR) spectroscopy (Bomen-MB-series 100, Hartman & Burn, Canada) over a range of 4000–500 cm^{-1} at a resolution of 8 cm^{-1} and 32 scans. FTIR spectra of polymer was collected at room temperature with applying the PCLF powder mixed with KBr and pressed disk.

Gel permeation chromatography (GPC) was performed using a GPC instrument (Agilant 1100) consisting of 10 μm PLgel column (104 Å, 103 Å, 102 Å, 500–400 kDa) to characterize the molecular weight and polydispersity of the synthesized macromere. In this experiment, determined molecular weight polystyrene was used as a calibration standard and reagent grade tetrahydrofuran (THF) was used as mobile phase eluting at flow rate of 1.0 mL/min. A 100 μL of PCLF in THF solution with concentration of 0.1 mg/mL filtered through a 0.2 μm filter was injected.

Thermal properties of synthesized polymer were measured using a differential scanning calorimeter (DSC 200 F3 Maia, NETZSCH) under a nitrogen gas flow rate of 50 mL/min. To preserve the same thermal history, each sample was first heated from room temperature to 100°C and cooled to −90°C at a cooling rate of 5°C/min. Then, next heating run was carried out over a temperature range of −90 to 100°C at a heating rate of 10°C/min. Glass transition temperature (T_g), melting temperature (T_m) and melting enthalpy (ΔH_m) of macromere were calculated from the DSC heating run.

Preparation of crosslinked electrospun PCLF:PCL nanofibrous scaffolds

For fabrication of PCLF:PCL nanofibers, the polymer solutions with concentrations in the ranges of 10–17% (w/v) were prepared by dissolving PCLF and PCL with weight ratios of 90:10, 80:20, and 70:30 in the mixture solvent of dichloromethane (DCM):DMF (4:1 v/v) and stirred overnight at room temperature. After optimization of electrospinning process and determination of the best concentration of electrospinning solution, BAPO as photo initiator was added to PCLF:PCL solution whereas the weight concentration of BAPO to PCLF was selected to be 1–6% and was stirred for 15 min to achieve a homogeneous solution. The mixed solution was loaded in to a 1 mL syringe fitted with a 23 G blunted stainless steel needle, which was connected to a high voltage power supply (15

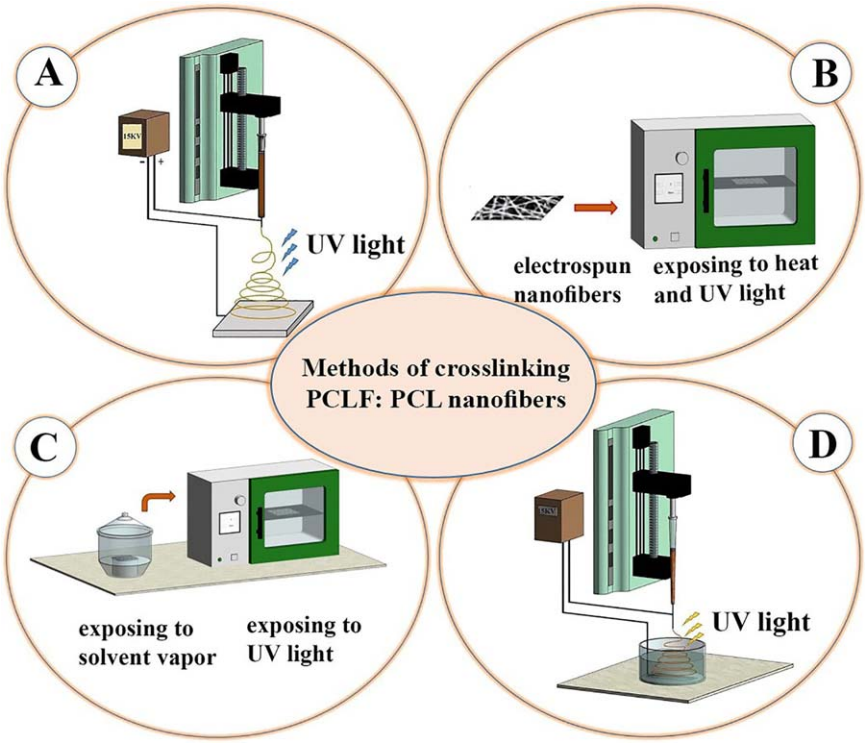

FIGURE 1. Crosslinking methods of PCLF:PCL nanofibers (A) *in situ* photo-crosslink (B) UV irradiated along with heating at 40°C (C) exposing to solvent vapor and then UV irradiation (D) *in situ* photo-crosslinking along with wet-electrospinning.

kV), pumped with flow rate of 0.2 mL/h and collected to aluminum foil placed in 15 cm distance from needle tip.

Different approaches including *in situ* photo crosslinking, UV irradiated along with heating at 40°C, exposing of PCLF:PCL nanofibers to solvent vapor and immediately irradiation under UV and *in situ* photo crosslinking along with wet electro spinning were examined for crosslinking of PCLF in the structure of PCLF:PCL nanofibers.

In situ photo-crosslinking method was examined by exposing of the jet traveling from the needle to the collector to the UV light ($\lambda = 315–380$ nm, 60 W) [Figure 1(A)].

Crosslinking of fabricated PCLF:PCL nanofibers containing BAPO as photo initiator was also performed by simultaneous application of UV light along with heating at 40°C in an isolating chamber [Figure 1(B)] for 30 min. In another approach, nanofibers mat containing photo initiator inserted in a desiccator saturated with acetic acid vapor (as solvent vapor) for 30 min and then irradiated under UV irradiated for 30 min [Figure 1(C)].

Finally, *in situ* photo crosslinking along with wet-electrospinning were used [Figure 1(D)]. Distilled water (as nonsolvent)/acetic acid (as solvent) (80:20 v/v) combination was used for electrospinning bath and nanofibers were collected on an aluminum foil which was placed inside the bath. The UV light was irradiated directly on the jet traveling from the tip of needle to the target that placed bottom of the electrospinning bath. The resultant electrospun nanofibers were then placed in a vacuum oven for 48 h at room temperature to remove any residual solvent and used for further characterization and cell culture experiments.

Characterization of electrospun nanofibers

The morphology of nanofibrous scaffolds was studied by Field Emission Scanning Electron Microscopy (SEM) (S 4160, HITACHI, Japan) and SEM (XL30, PHILIPS, Netherlands) at an accelerating voltage of 20 kV. Before observation, the nanofibers were coated with gold using a sputter coater (SBC 12, Japan (. The diameter of the fibers was measured from the SEM micrographs using image analysis software (Digimizer, Medcalc Software Company).

FTIR analysis applied to nanofibers before and after crosslink process to confirm the crosslink occurrence, as described in Characterization of synthesized PCLF section.

To investigate the effect of the crosslinking on the thermal properties of nanofibrous scaffolds, DSC (200 F3 Maia, NETZSCH) was performed under the conditions mentioned in Characterization of synthesized PCLF section.

X-ray diffraction was used to evaluate the crystallinity of crosslinked and noncrosslinked PCLF:PCL nanofibers. An X-ray diffractometer (XRD, Philips model Xpert MPD, The Netherlands) emitting CuKα radiation with a wavelength of 1.54 Å, operating at 40 kV and 30 mA was used to collect data. For recording of data, angles ranging from 5 to 60° were covered and scans were taken with a step size of 0.04°and held for 1.0 s.

Sol fraction extraction and swelling ratio experiment were performed on the crosslinked samples. The samples were precisely weighed (W_0) and immersed in CH_2Cl_2 under gentle shacking for 72 h. After this period, the samples were taken out and weighed immediately after blotted (W_s). Then samples were dried in vacuum oven at room temperature and weight of samples was measured (W_d). The

swelling ratio and sol fraction percent of samples were calculated using the Eqs. (1) and (2), respectively,

$$\text{Swelling ratio}\,(\%) = \frac{W_s - W_d}{W_d} \times 100 \quad (1)$$

$$\text{Sol fraction}\,(\%) = \frac{W_0 - W_d}{W_0} \times 100 \quad (2)$$

All tests were repeated three times for each sample and the results were reported as mean ± standard deviation (SD).

Mechanical properties characterization of the electrospun nanofibrous scaffolds was carried out using a uniaxial tensile testing machine (Zwick 1446–60, Germany) by applying a 20 N load cell at a crosshead speed of 10 mm/min at ambient conditions. For mechanical test, samples were cut into rectangular shape with dimensions of 50 × 10 mm^2 and mechanical properties were measured for samples. At least five samples were tested for each type of the electrospun nanofibrous scaffolds.

Dynamic mechanical analysis (DMA) analysis of the electrospun nanofibrous scaffolds were performed using a DMA 242C instrument (NETZSCH, Germany). Temperature scans at frequencies rang of 0.6–2 Hz were carried out. The samples were tested at temperature range of −100 to 90°C at a heating rate of 3°C/min under nitrogen atmosphere. The analysis was carried out under oscillatory tension mode. The storage modulus (E'), loss modulus (E'') and tan δ values were recorded against temperature at different frequencies.

Degradation studies were performed by incubating the electrospun PCLF:PCL nanofibrous scaffolds ($n = 3$ per time point) in 24-well plate containing 1 mL of a phosphate buffered saline (PBS, pH 7.4) at 37°C until 60 days. At each time point (15, 30, 45, 60 days), the samples were removed, washed with distilled water and subsequently dried in a vacuum oven at room temperature for 48 h and then weighed for calculation of the weight loss. Moreover, SEM images were used for understanding the changes in morphology of nanofibers during degradation period.

For evaluation of wettability of PCLF:PCL nanofibers, the contact angle was measured by a video contact angle system (OCA 15 plus, Dataphysics) and droplet size of 4 μL. Three samples were used for each test and the average value was reported with standard deviation (± SD).

Cell studies

Cell culture of 3T3 fibroblasts. NIH 3T3 mouse fibroblasts (ATCC, UK) were cultured in DMEM containing 10% fetal bovine serum, 50 U/mL penicillin and 50 U/mL streptomycin. The medium was replaced every 3 days and cultures were maintained in a tissue culture incubator at 37°C with 5% CO_2. After reaching about 80% confluence, cells were detached by 0.05% trypsin/0.05% ethylenediaminetetraacetic acid (EDTA). Cells were seeded onto scaffolds at a density of 5000 cells/cm^2 and were cultured in incubator at 37°C with 5% CO_2.

Metabolic activity and proliferation of 3T3 fibroblasts. Cell viability and metabolic activity in response to different substrates of tissue culture polystyrene (TCP) cover slip, crosslinked and noncrosslinked PCLF:PCL nanofibers were measured using 3-(4,5-dimethylthiazol-2-yl)-5-(3-carboxymethoxyphenyl)-2-(4-sulfophenyl)-2H-tetrazolium (MTS) cytotoxicity assay, according to the manufacturer's instructions. Cells were seeded at a density of 5000 cells/$cm^2$and the cell activity was evaluated during a 7-day period. On days 1, 3, and 7, the cell seeded sheets were punched in diameter of 10 mm (fitting the 24-well plates), were transferred to 24 well plates, and washed with PBS. Then 500 μL of culture medium was added to each well. Consequently, 100 μL of MTS solution was added to each well. Cells were maintained for an additional 4 h in a humidified incubator at 37°C and 5% CO_2. Finally 100 μL of the solution in each well was transferred to 96 well plate, and the absorbance was read at 490 nm in a spectrophotometer Microplate Reader (wallac VICTOR3 1420 multilable counter, PerkinElmer). The measured absorbency was considered as cell metabolic activity on each substrate in different time points. This was done in triplicates followed by calculations of mean values and standard deviations.

Cell morphology. The morphology of cell-seeded scaffolds was studied with the help of SEM after 1 and 7 days of cells seeding. Specimens were fixed overnight in 2.5% glutaraldehyde in cacodylate buffer and washed with cacodylate buffer. Subsequently, samples were dehydrated with increasing concentrations of ethanol (30, 50, 70, 90, and 100%) for 10 min each. Finally, the constructs were treated with hexamethyldisilazane to further water extraction. The dehydrated constructs were maintained in desiccators equipped with a vacuum for overnight air drying. After sputter-coating with Platinum, SEM was used to observe surface of scaffolds, as well as morphological study of 3T3 fibroblasts grown on sheets after 1 and 7 days of cell culture.

Statistical analysis

All measured values are expressed as mean ± SD. Statistical analysis of all data was carried out by one-way analysis of variance and student's *t test*. A value of $p \leq 0.05$ was considered statistically significant.

RESULTS

Synthesis and characterization of synthesized PCLF

PCLF macromere was synthesized by the polycondensation reaction between PCL diol and fumaryl chloride in the presence of K_2CO_3 as catalyst (Figure 2). Figure 3(A) shows the GPC graph and from the results it can be concluded that the values of number-average molecular weight (Mn), weight-average molecular weight (Mw), and polydispersity index of synthesized PCLF in the present study are 13,284, 26,560 g mol^{-1} and 1.1, respectively.

The thermal behavior of synthesized PCLF was evaluated by DSC technique. Figure 3(B) illustrates the DSC thermogram of synthesized PCLF indicating a T_g at −55.7°C and T_m at 39.6. According to linear correlation between crystallinity and enthalpy, the crystallinity of PCLF (χ_c) was calculated to be 30.8% using Eq. (3):[16]

$$\chi_c = \left[\Delta H_m / \varnothing \Delta H_m^c\right] \times 100 \quad (3)$$

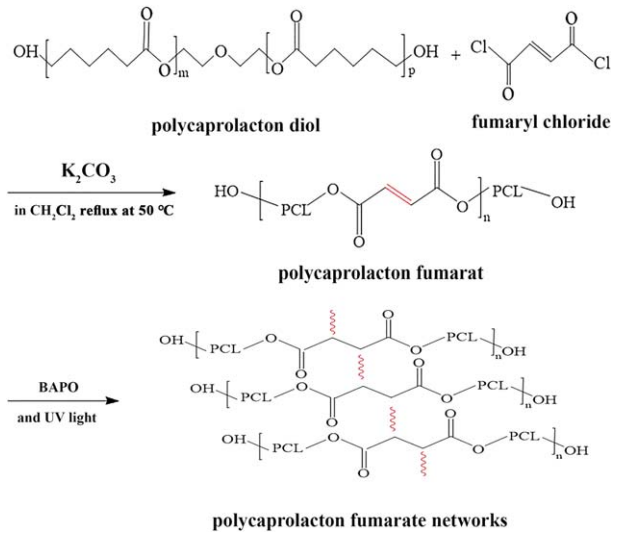

FIGURE 2. Schematic illustration of PCLF synthesis and its crosslinking reaction.

where; ΔH_m is the heat of fusion of PCLF (39.8 J/g) obtained from DSC analysis, $\Delta H_m^c$is heat of fusion for completely crystalline PCL (135 J/g) and the composition ∅ of PCL was considered 98.1%.[13,16]

Figure 3(C) shows the FTIR spectra of PCL and PCLF. Asymmetrical C–O–C stretching band and the absorption band of C=O vibration of PCL and fumarate are appeared at 1100 and 1730 cm^{-1} in both spectrum of PCL and PCLF, respectively. Absorption bands with peak positions at 2944 and 2870 cm^{-1}, due to the asymmetrical and symmetrical stretching of the methylene groups of PCLs, held in common to the spectrum of PCL before and after the reaction with fumaryl chloride. Hydroxyl absorption observed at 3440 cm^{-1} for PCL and PCLF. Comparing the spectra of PCL diol and PCLF, the presence of absorption band at 1640 cm^{-1} confirms the formation of fumaryl group in the structure of synthesized PCLF.

Fabrication of electrospun nanofibers

In order to optimize the electrospinning of PCLF:PCL solution based on maximum possible contribution of PCLF, PCLF:PCL solutions with different weight ratios of 90:10, 80:20, and 70:30 and different concentration of 10–17% were prepared. Our results suggested the successful formation of uniform and bead-free nanofibers was achieved at concentration of 17%, and weight ratio of 70:30, leading to fiber diameters of 1915.79 ± 389 nm [Figure 4(A)].

Crosslinking of PCLF:PCL nanofibers

We applied different crosslinking techniques mentioned in the material and method section for crosslinking of nanofibers, and finally the optimum condition of crosslinking was selected in viewpoints of mechanical properties along with preservation of morphology of nanofibers.

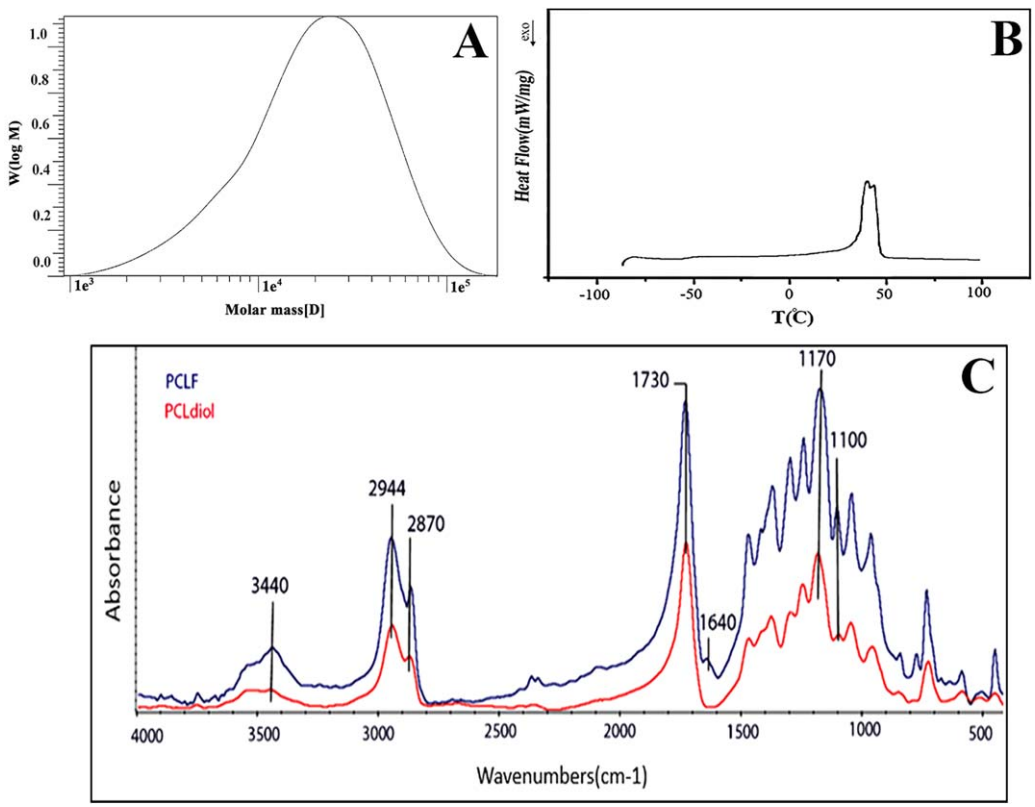

FIGURE 3. Characterization of synthesized PCLF (A) GPC chromatograms of PCLF (B) DSC curve of synthesize PCLF (C) FTIR spectra of synthesized PCLF and its precursor (PCL diol).

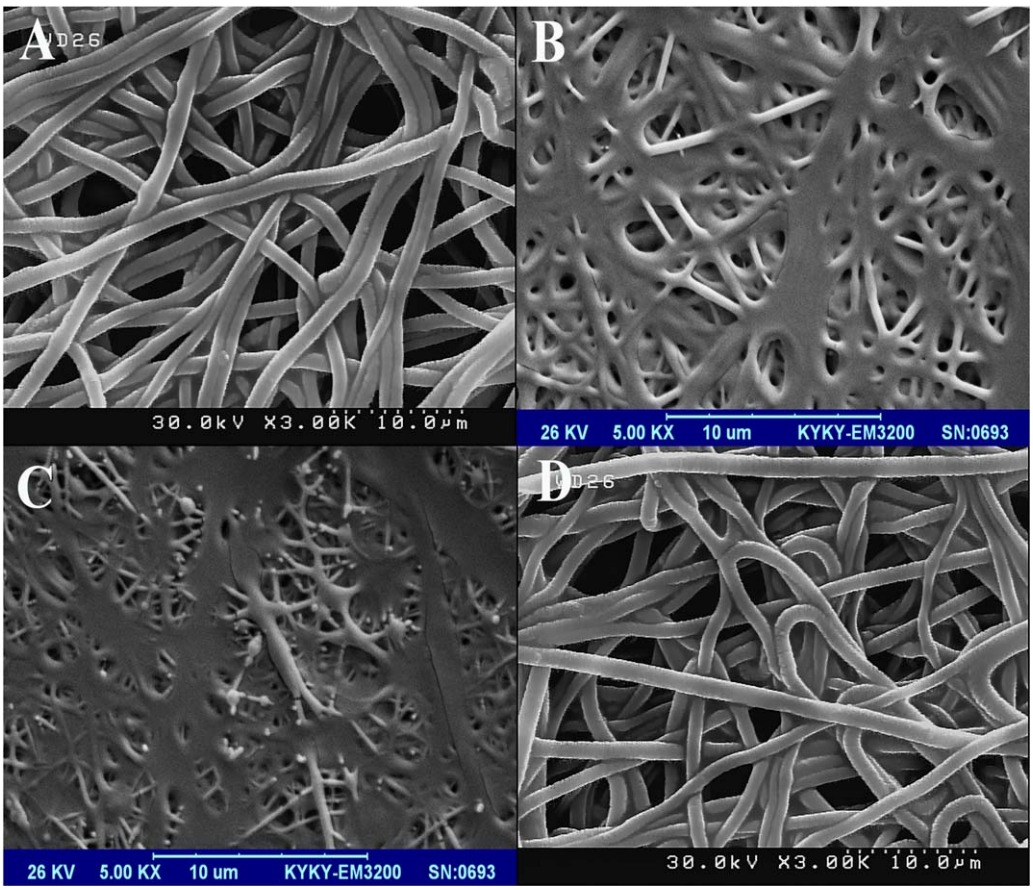

FIGURE 4. SEM image of (A) noncrosslinked nanofibers fabricated whit PCLF:PCL weigh ratio of 70:30 and concentration of 17% w/v. SEM images of crosslinked nanofibers with different methods (B) UV irradiation along with heating of nanofibers at temperature of 40°C (C) exposing to solvent and immediately transferred to UV radiation chamber (D) *in situ* photo-crosslinking along with wet electrospinning technique.

Table I shows the mechanical properties of crosslinked nanofibers using the different methods. No difference was observed for the mechanical properties of the noncrosslinked nanofibers and the nanofibers that were fabricated with electrospinning along with *in situ* photo crosslinking (data not shown). According to Table I, compared with UV irradiation singly, applying of heating and exposing to solvent vapor beside on UV irradiation was found to improve the mechanical properties. However, as shown in Figure 4(B,C) the morphology of nanofibers produced by methods mentioned in the Figure 1(B,C), were deformed during crosslinking.

According to mechanical properties results and morphology of fabricated nanofibers, the *in situ* photo crosslinking along with wet electrospinning technique [method relevant to Figure 1(D)] was found to be the most appropriate method and was chosen as optimum condition for crosslinking of PCLF:PCL nanofibers in this study. In addition, comparison of two spectra in Figure 6(D) show that the peak of fumaryl group (at 1640 cm^{-1}) has become broader after crosslinking which confirms the participation of double carbon bands of fumaryl group in the crosslink process. Compared to conventional PCLF:PCL electrospun nanofibers, the average diameter of wet electrospun nanofibers was slightly reduced to 1298.96 ± 241 nm.

For improvement of mechanical properties of PCLF:PCL nanofibers during *in situ* photo crosslinking along with wet

TABLE I. Mechanical Properties of Crosslinked Nanofibers with Different Methods

	Crosslinking Methods			
Mechanical Properties	Non-crosslinked[b]	UV + (40°C)	sv[a]	UV + Wet Electrospinning[b]
Tensile strength (MPa)	1.9 ± 0.5	2.9 ± 0.4	2.5 ± 0.5	0.2± 0.0
Strain at break (%)	14.4±5.3	24.0±2.3	25.0±3.3	114.5± 3.9
Young's modulus (MPa)	13.9±1.4	22.8±3.8	16.38±2.0	0.6± 0.1

[a] sv, solvent vapor.
[b] Results reported for optimum sample (5% BAPO).

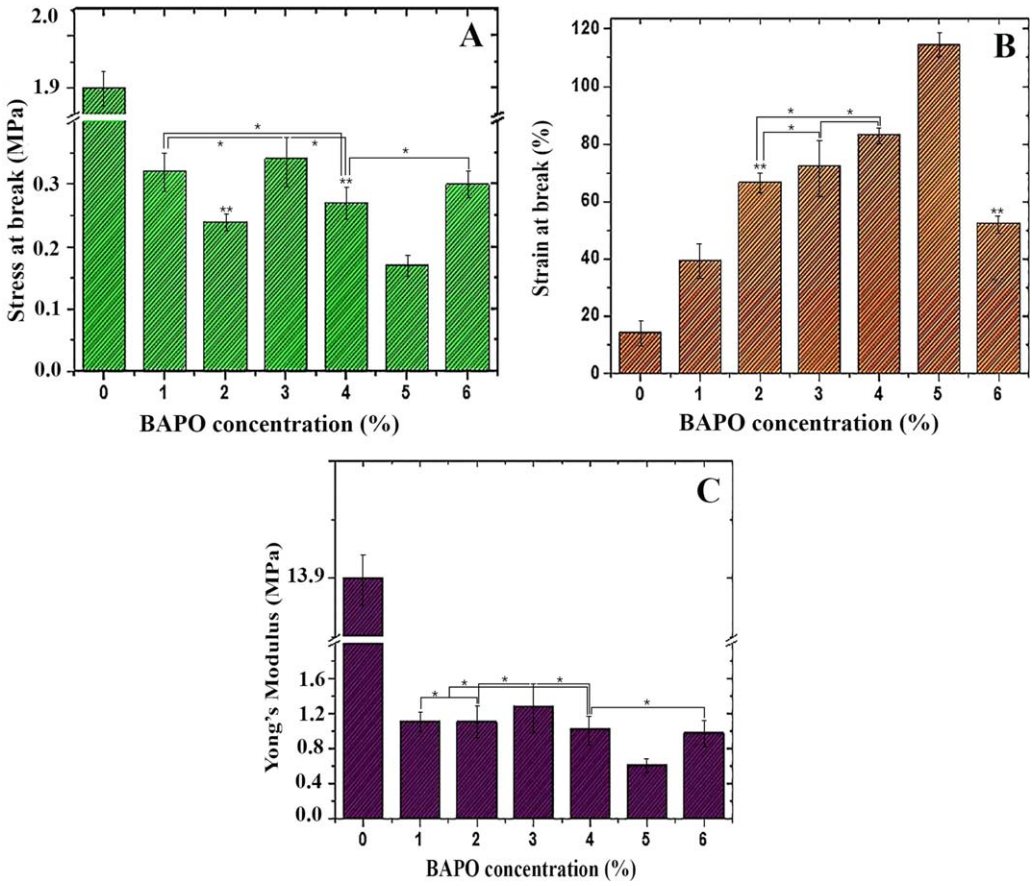

FIGURE 5. Mechanical properties (A) stress at break (MPa) (B) strain at break (%) (C) Young's modulus (MPa) of PCLF:PCL nanofibers at different BAPO concentrations. Data are reported as mean ± SD. ** and * No significant different at $p \leq 0.05$.

electrospinning, different concentration of BAPO was used. Figure 5 shows mechanical properties of wet electrospun nanofibers with different BAPO concentrations. As can be seen in this figure, strain of nanofibers increased with increasing of BAPO concentration whereas tensile strength and Young's modulus decreased. Finally, concentration of 5% was selected as optimum concentration for final sample fabrication. In total, optimum PCLF:PCL nanofibers were fabricated by *in situ* photo crosslinking along with wet electrospinning technique with 5% concentration of BAPO.

Characterization of electrospun crosslinked PCLF:PCL nanofibers

Thermal properties and crystalline structure of nanofibers. To investigate the effect of crosslinking on the thermal properties and crystallinity of nanofibers, DSC test was performed on nanofibers before and after crosslinking [Figure 6(A)]. As reported earlier,[16] PCLF is a semicrystalline polymer with molecular weight-dependent T_m. According to the results that listed in Table II, no noticeable difference was observed in T_m of nanofibers before and after crosslinking. T_g, ΔH_m and $\chi_c$was found to decrease from −36.9°C, 45.6 J/g, and 34.6% for noncrosslinked nanofibers to −50.8°C, 19.7 J/g, and 14.9% for crosslinked nanofibers, respectively.

The XRD was used to investigate the crystalline structures of noncrosslinked and crosslinked nanofibers. Figure 6(B,C) represent the (110), (111), (200), and (210) diffraction peaks at 2θ = 20.2, 21.4, 22.0, 23.7, and 30.0, respectively, which refer to their precursor PCL diol.[25,26] The intensities of the mentioned diffraction peaks of the noncrosslinked PCLF were greater than those of the crosslinked PCLF, indicating higher degree of crystallinity in the noncrosslinked nanofibers compared to crosslinked nanofibers which is in accordance with the DSC results.

Gel fraction and swelling ratio of crosslinked nanofibers. PCLF swells in organic solvents such as dichloromethane significantly[16] and the swelling ratio of crosslinked PCLF nanofibers indicates the relative crosslink density whereas less crosslinked PCLF nanofibrous scaffold represents more swelling ratio when immersed in solvent.[27] Figure 7(A) compares the swelling ratio of crosslinked PCLF nanofibers fabricated with different weight ratios of BAPO:PCLF. As can be seen, by increasing the amount of BAPO in the structure of nanofibers, the swelling ratio reduced, which can be attributed to the increase of the crosslink density.

Figure 7(B) illustrates sol fraction of nanofibers with different amount of BAPO. As can be observed from this figure,

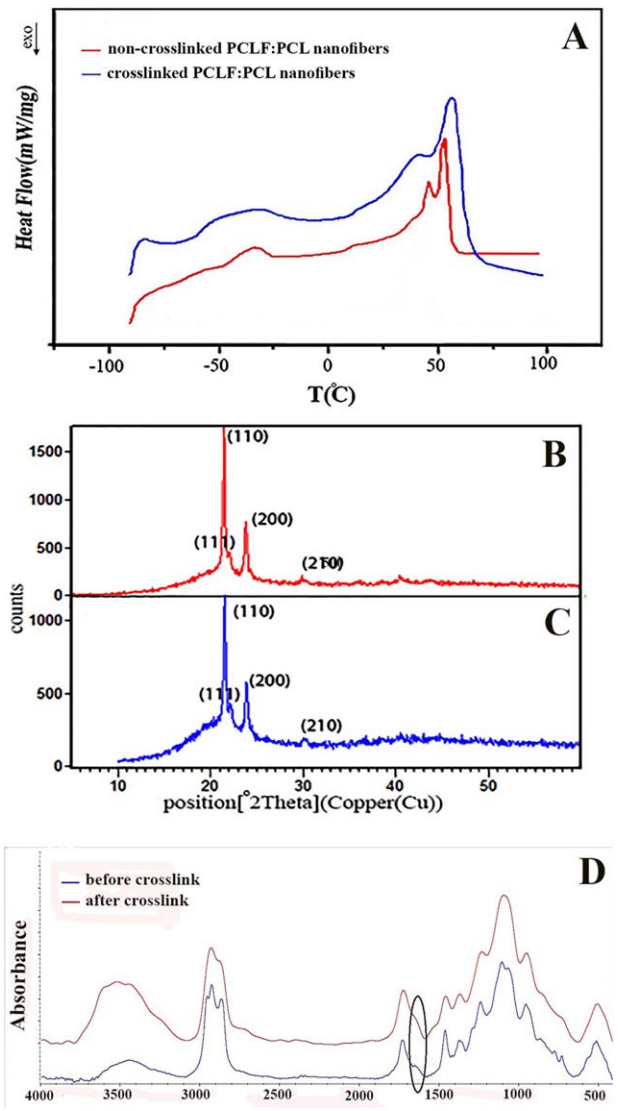

FIGURE 6. A: DSC curves of noncrosslinked and crosslinked PCLF:PCL nanofibers and (B) XRD pattern of noncrosslinked and (C) XRD pattern of crosslinked PCLF:PCL nanofibers (D) FTIR spectra of PCLF:PCL nanofibers before and after crosslinking.

by increasing BAPO content in the structure of nanofibers, sol fraction decreases due to increasing of crosslink density which is consistent with the results of swelling ratio.

Hydrophilicity and *in vitro* biodegradation

Contact angle of water on the PCLF:PCL nanofibers was measured for evaluating surface wettability. The contact angle for crosslinked PCLF:PCL nanofibrous scaffold was $80 \pm 2°$ [Figure 9(A)] which is in agreement with the value of $85 \pm 3°$ reported earlier for crosslinked PCLF film indicating the relative hydrophilic property of crosslinked nanofibers.[28]

Hydrolytically degradation of crosslinked PCLF:PCL nanofibrous scaffold was examined by morphological changes and weight loss of nanofibers in PBS at 37°C. Morphological changes of electrospun PCLF:PCL nanofibers during *in vitro* degradation after 30 and 60 days of incubation in PBS solution at 37°C was studied by SEM imaging and is shown in Figure 8. No significant morphological changes were observed in electrospun PCLF:PCL nanofibers during this time and just a little swelling in the nanofibers was observed. Moreover, the weight loss of 18.5% after 60 days was observed [Figure 9(B)] which is not noticeable and it is consistent with SEM results.

TABLE II. Thermal Properties of Crosslinked and Noncrosslinked PCLF:PCL Nanofibers

	Thermal Properties			
Sample	T_g (°C)	T_m (°C)	ΔH_m (J/g)	χ_c (%)
Noncrosslinked PCLF:PCL	−36.9	56.3	45.6	34.6
Crosslinked PCLF:PCL	−50.8	57.9	19.7	14.9

Dynamic mechanical analysis

The viscoelastic behavior of PCLF:PCL nanofibers was evaluated by measuring the storage modulus (E'), loss modulus (E'') and the loss factor (tan $\delta = E''/E'$) using DMA at room temperature (25°C) and body temperature (37°C) and in the frequency range from 0.6 to 2 Hz. At the frequencies of 0.6–2 Hz, the storage modulus, the viscous modulus and the loss factor of scaffold decreased by increasing the temperature from 25 to 37°C. However, at both temperature and in the frequency range of 0.6–2 Hz, the value of the storage modulus was found to be much higher than the viscous modulus suggesting that elastic nanofibers were developed. As shown in Figure 10 the storage modulus increased simultaneous with increasing frequency over the test indicating the ability of the scaffold to store energy under cyclic load.[29]

Cell culture study

Figure 11 shows the MTS result of cells seeded on crosslinked and noncrosslinked PCLF:PCL and TCP as control. As can be observed from this figure, significant levels of proliferation occurred during the one week culture time. This trend is similar for both crosslinked and noncrosslinked samples. No significant difference was observed between proliferation of cells on nanofibers before and after crosslinking.

Figure 12 shows SEM micrographs of cells seeded on noncrosslinked and crosslinked PCLF:PCL nanofibrous scaffolds after 1 and 7 days of cell seeding. As can be seen in this figure, cells proliferate and spread well on both scaffolds.

DISCUSSION

The aim of this study was to present an elastomer nanofibrous scaffold from PCLF, characterize it and study its potential for application in soft tissue engineering field. PCLF is a biodegradable, biocompatible and self-crosslinkable unsaturated linear polyester. It also has been shown that crosslinking of PCLF imposes elastomeric properties to the fabricated structure.[13,30] To create elastomer nanofibrous scaffold, PCLF was synthesized and

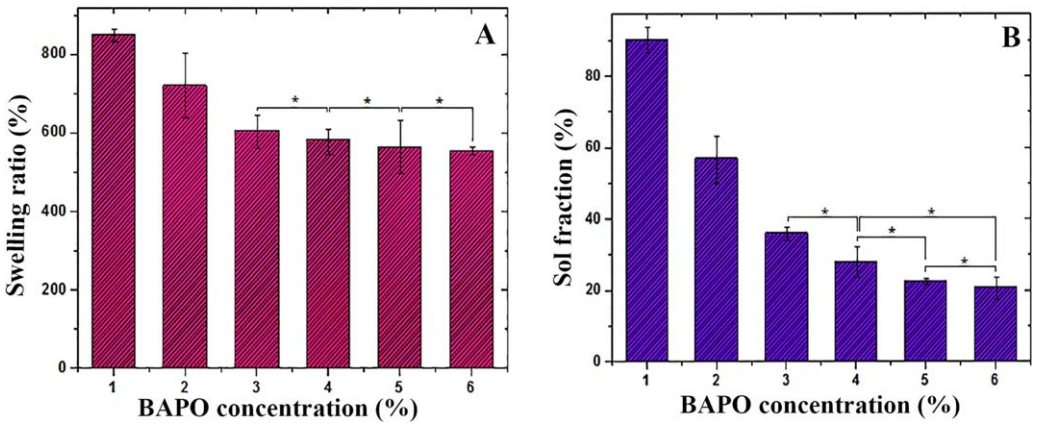

FIGURE 7. A: Swelling ratio and (B) sol fraction of crosslinked PCLF:PCL nanofibers. Data are reported as mean ± SD. *No significant different at $p \leq 0.05$.

characterized during this study FTIR analysis indicated the presence of fumaryl group as characteristic absorption band in the structure of synthetized PCLF[13,30] [Figure 3(C)]. DSC results obtained during this study were similar to those reported in previous studies[13,30] again confirming that synthetize of PCLF was performed well in this research.

According to morphological similarity of electrospun nanofibers with native extra cellular matrix and high surface area to volume ratio of nanofibers, electrospun nanofibrous scaffolds were fabricated.[31] Although there are some publications on fabrication of PCLF scaffolds for nerve and bone tissue engineering,[28,32–34] there is no study on PCLF-based nanafibrous scaffolds for soft tissue engineering. Electrospinning of pure PCLF was a great challenge in this study, as no continuous fiber formation was observed from pure PCLF solution. It is likely due to low molecular weight of synthetized PCLF (13,284 g/mol). In our study, PCLF was blended with PCL and electrospun PCLF:PCL nanofibers were fabricated with different weight ratios of 90:10, 80:20, and 70:30. No uniform and bead-free nanofibers were

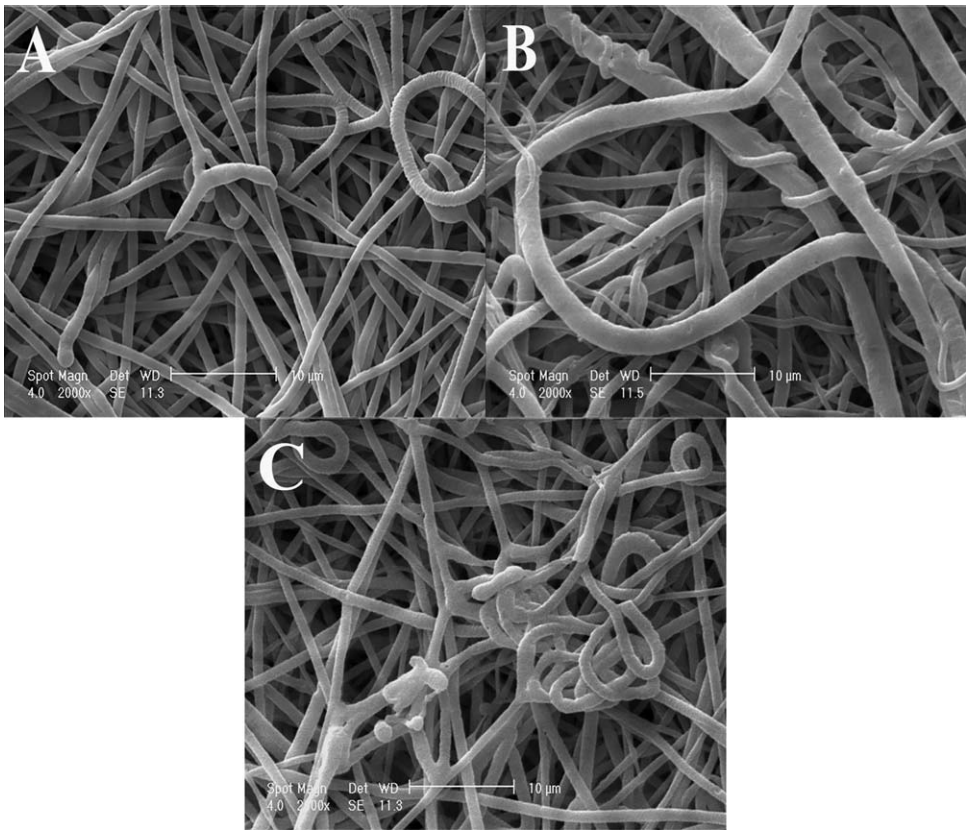

FIGURE 8. Morphology of (A) PCLF:PCL nanofiber before biodegradability test, (B) PCLF:PCL nanofiber after 30 days biodegradability test, and (C) PCLF:PCL nanofiber after 60 days biodegradability test.

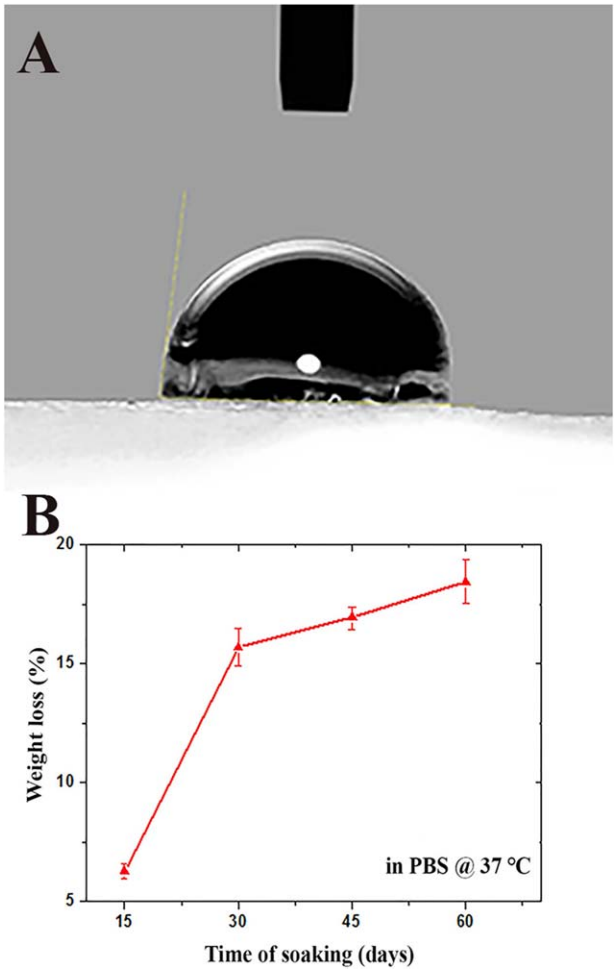

FIGURE 9. A: Contact angle of crosslinked PCLF:PCL nanofibers. B: Weight loss of crosslinked PCLF:PCL nanofibers in PBS at 37°C.

achieved when weight ratios containing >70% PCLF. Hence, PCLF:PCL (70:30) solution was selected as optimum condition for electrospinning.

In this study, different approaches were used for crosslinking of PCLF:PCL nanofibers. Recently, *in situ* photo-

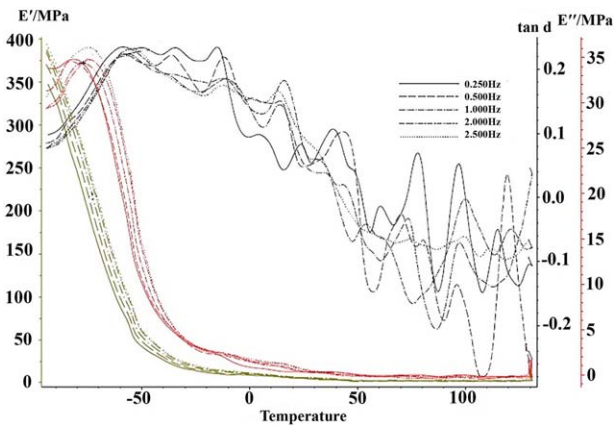

FIGURE 10. Dynamic mechanical properties of scaffold. Storage modulus (green curve), loss modulus (red curve), and loss factor (black curve).

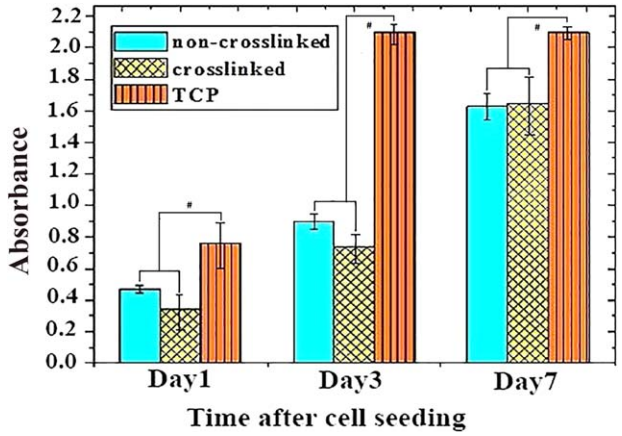

FIGURE 11. Prolifration of NIH 3T3 mouse fibroblasts on PCLF:PCL nanofibrous scaffold after 1, 3, and 7 days of cell seeding. Data are reported as mean ± SD. #Significant different at $p \leq 0.05$.

crosslinking has been used for crosslinking of different polymers such as gelatin, poly(vinyl alcohol), methacrylated polycarbonate and hybrids of polyurethane/methacrylated poly(ethylene glycol) during electrospinning.[35–38] In the mentioned studies, the methacrylate group was activated when exposed to light, and by creating crosslinking bonds (with opening of double carbon bonds) produced from elastomeric properties in fabricated nanofibers. Since the mechanism for creating crosslinking bonds by the fumaryl group is similar to methacrylate, *in situ* photo-crosslinking was examined for crosslinking of PCLF in this research and results (mechanical properties and dissolution test) showed that no crosslinking was occurred in the structure of nanofibers. It should be noted that in the previous studies the crosslinking of PCLF was performed by exposing of PCLF solution to UV radiation[35–37] while during electrospinning, the nanofibers solidify immediately. Moreover, the crosslinking reaction of fumarate-based macromeres is very slow due to the steric hindrances constrained from the fumarate double bonds that positioned with their arms as trans isomer along with the PCLF backbone that restrict the movement of the macroradicals generated by the PCLF chains.[39] According to aforementioned reasons of reduction chain mobility in the solid state (nanofibers) relative to the liquid state (film casting solution) and steric hindrances, it can be concluded that *in situ* photo-crosslinking is not an appropriate method for crosslinking of PCLF:PCL nanofibers. The most challenging issue of this research was crosslinking of nanofibers in solid state.

As we aimed to increase the chain mobility for exposure fumaryl groups, different postelectrospinning crosslinking methods including UV irradiation along with heating of nanofibers at 40°C for 30 min were also designed [Figure 1(B)]. No noticeable changes in mechanical and dissolution properties of nanofibers were observed with nanofibers exposed to UV radiation alone, revealing the ineffectiveness of this method for crosslinking of nanofibers. Although dissolution and mechanical properties of nanofibers were improved by application of heating along with UV radiation,

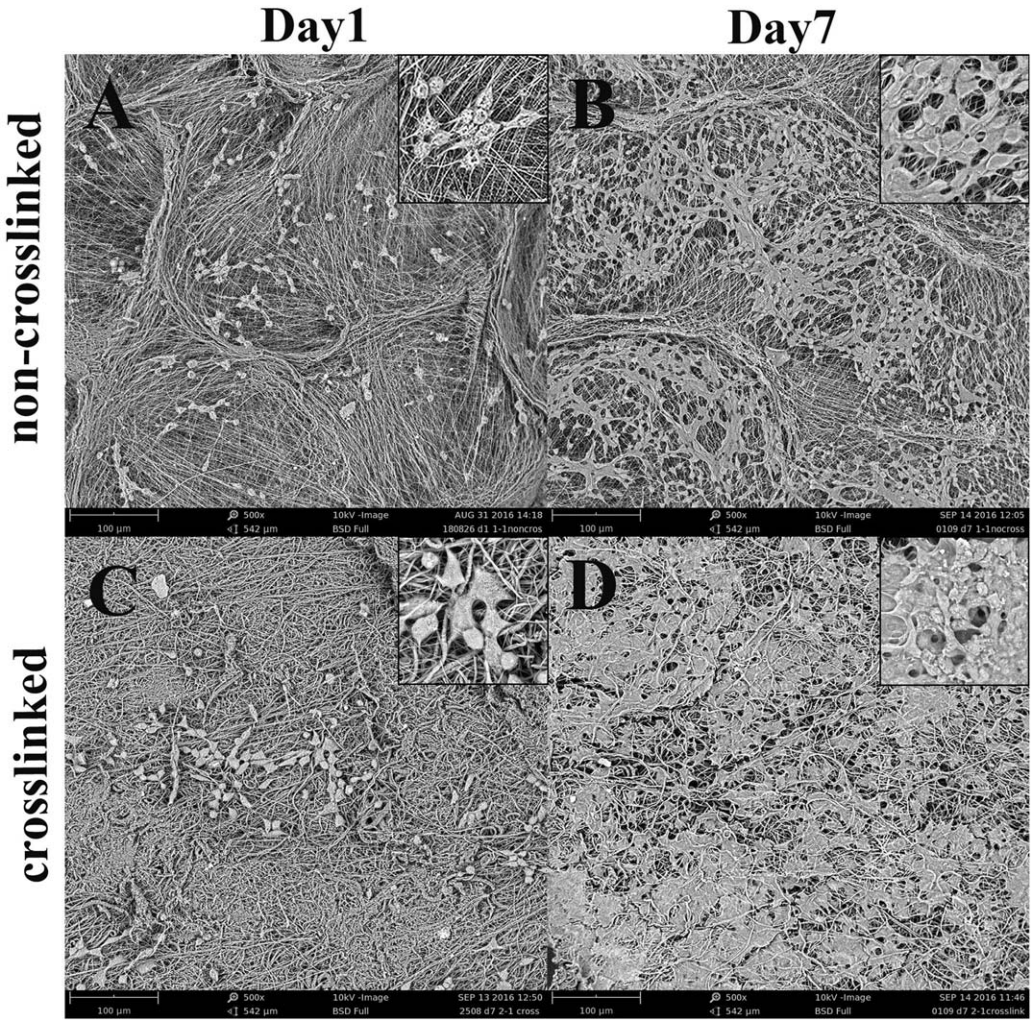

FIGURE 12. Morphology of NIH 3T3 mouse fibroblasts on noncrosslinked PCLF: PCL nanofibers (A) after 1 day, (B) after 7 days of cell culture and crosslinked PCLF:PCL nanofibers (C) after 1 day, (D) after 7 days of cell culture.

the observable changes in morphology of nanofibers was seen in SEM images of nanofibers [Figure 4(B)] which is likely due to melting of nanofibers. As improvement of mechanical properties of nanofibers was observed by heating along with UV irradiation, it can be concluded that heating causes the increasing of chain mobility of polymer and it facilitates the crosslinking of nanofibers.

Due to unwanted morphological changes in nanofibers after heating, electrospun nanofibers were exposed to solvent vapor for preserving polymer chain mobility and immediately transferred to UV radiation chamber [Figure 1(C)]. Although improvement in mechanical and dissolution properties of nanofibers was distinguished, deterioration of morphology of nanofibers was observed in this method as well [Figure 4(C)] which is likely due to dissolution of nanofibers in solvent vapor.

Regarding to retarding of solidification during wet electrospinning, *in situ* photo crosslinking during wet electrospinning was examined [Figure 1(D)]. A combination of solvent and nonsolvent (water [as nonsolvent of PCLF]:acetic acid [as solvent of PCLF]) with volume ratio of 80:20 was used in coagulation bath for postpone solidification of nanofibers and longer duration of polymeric jet in gel-state leading to more chain mobility which encourages crosslinking of nanofibers. SEM images illustrated that morphology of crosslinked nanofibers fabricated from wet electrospinning and mentioned coagulation bath, was preserved [Figure 4(D)].

For the optimization of wet electrospinning process, different amounts of photoinitiator (2–6%) was added to electrospinning solution and nanofibers were fabricated. As can be observed from Figure 5(B), nanofibers with 5% w/w of BAPO showed the highest strain at break (114.5 $\pm$ 4%). Increasing of BPAO content from 5 to 6% in electrospinning solution, was found to decrease the strain at break to 52.30 $\pm$ 1.57 and increase the Young's modulus and stress at break which is probably due to high density of crosslinking. Then concentration of 5% of BAPO was selected as optimum condition. As shown in Figure 7, by increasing the amount of BAPO in the structure of nanofibers, the swelling ratio and sol fraction reduced due to increasing of crosslink density which is consistent with mechanical properties results.

Surface wettability that is affected by the surface energy, is one of the biomaterial features that tune initial cell adhesion and behavior.[28] The contact angle obtained for PCLF:PCL nanofibrous scaffold in this study was $80 \pm 2^{\circ}$ wich is lower than the contact angle of PCL nanofibers (109–134°) reported in previous studies. It can be concluded that incorporation of fumaryl group in the structure of nanofibers, improve the hydrophilicity which may be due to the presence of carbonyl groups of fumaryl segments in PCLF backbone macromers.

Slow degradation was observed for PCLF:PCL nanofibers during 60 days incubation and the results are consistent with other studies (Figures 8 and 9).[28]

DMA analysis was performed on the PCLF:PCL nanofibrous scaffold for examination of viscoelastic response of PCLF:PCL scaffold to cyclic deformation. DMA results (Figure 10) indicate the viscoelastic behavior of PCLF:PCL nanofibrous scaffolds. The viscoelastic behavior was evaluated by measuring the storage and loss modulus and our results showed much higher values of storage modulus compared to loss modulus indicating elastomeric behavior of scaffold fabricated in this study. For both temperatures (25 and 37°C), the elastic modulus increased continuously over the tested frequency range.[40]

As observed from Table I, tensile strength of PCLF:PCL nanofibrous scaffolds prepared with 5%w/w BAPO is close to the mammalian left ventricle (0.15 MPa in a canine model)[41] and Young's modulus value is in the range of Young's modulus of rat and human myocardium (10 kPa to 1 MPa). Furthermore, the PCLF:PCL nanofibrous scaffold showed elastic properties in the frequency range from 0.6 to 2 Hz which is in the range of at the rest heart frequency until physiological frequency interval of beating heart.[20] Therefore, it can be suggested that the produced substrate can be a potential candidate for the soft heart tissue. Of course, it is worth noting that investigation this capability requires supplementary *in vitro* and *in vivo* testing.

Cell spreading and proliferation was observed by SEM images on both crosslinked and noncrosslinked PCLF-PCL nanofibers confirming the MTS results. *In vitro* cell culture results revealed the biocompatibility of samples even after crosslinking using BAPO which make this scaffold suitable for soft tissue engineering.

CONCLUSION

Electrospun PCLF:PCL (70:30 w/w) nanofibrous scaffold was fabricated and different approaches were tested for crosslinking of PCLF within the nanofinbers structure. A novel *in situ* photo crosslinking along with wet electrospinning method was selected for crosslinking of nanofibers due to desirable elastic properties of the nanofibers after crosslinking. PCLF:PCL (70:30 w/w) nanofibers with 5% (w/w) BAPO were selected as optimum sample for cell culture experiments and *in vitro* cell culture studies revealed the biocompatibility of resultant nanofibers. The elastic behavior and the mechanical properties of PCLF:PCL nanofibers indicates that PCLF:PCL nanofibrous scaffolds fabricated in this study can be a potential candidate for applying in soft tissue repair and regeneration.

ACKNOWLEDGEMENTS

This work was supported by grants from Danish Research Council Foundation (4093-00282A and 4217-00048A) and Isfahan University of Technology-Isfahan-Iran.

REFERENCES

1. Costa RR, Costa AMS, Caridade SG, Mano JF. Compact saloplastic membranes of natural polysaccharides for soft tissue engineering. Chem Mater 2015;27(21):7490–7502.
2. Okabe K, Yamada Y, Ito K, Kohgo T, Yoshimi R, Ueda M. Injectable soft-tissue augmentation by tissue engineering and regenerative medicine with human mesenchymal stromal cells, platelet-rich plasma and hyaluronic acid scaffolds. Cytotherapy 2009;11(3): 307–316.
3. Brett E, Chung N, Leavitt WT, Momeni A, Longaker MT, Wan DC. A review of cell-based strategies for soft tissue reconstruction. Tissue Eng 2017;23:336–346.
4. Xu H, Cai S, Sellers A, Yang Y. Intrinsically water-stable electrospun three-dimensional ultrafine fibrous soy protein scaffolds for soft tissue engineering using adipose derived mesenchymal stem cells. RSC Adv 2014;4(30):15451–15457.
5. Xu H, Cai S, Sellers A, Yang Y. Electrospun ultrafine fibrous wheat glutenin scaffolds with three-dimensionally random organization and water stability for soft tissue engineering. J Biotechnol 2014;184:179–186.
6. Bat E, Zhang Z, Feijen J, Grijpma DW, Poot AA. Biodegradable elastomers for biomedical applications and regenerative medicine. Regener Med 2014;9(3):385–398.
7. Xu B, Li Y, Fang X, Thouas GA, Cook WD, Newgreen DF, Chen Q. Mechanically tissue-like elastomeric polymers and their potential as a vehicle to deliver functional cardiomyocytes. J Mech Behav Biomed Mater 2013;28:354–365.
8. Li Y, Thouas GA, Chen Q, Novel elastomeric fibrous networks produced from poly(xylitol sebacate) 2:5 by core/shell electrospinning: Fabrication and mechanical properties. J Mech Behav Biomed Mater 2014;40:210–221.
9. Partlow BP, Hanna CW, Rnjak-Kovacina J, Moreau JE, Applegate MB, Burke KA, Marelli B, Mitropoulos AN, Fiorenzo G Omenetto, David L Kaplan. Highly tunable elastomeric silk biomaterials. Adv Funct Mater 2014;24(29):4615–4624.
10. Gao J, Crapo PM, Wang Y. Macroporous elastomeric scaffolds with extensive micropores for soft tissue engineering. Tissue Eng 2006;12(4):917–925.
11. Pêgo AP, Poot AA, Grijpma DW, Feijen J. Biodegradable elastomeric scaffolds for soft tissue engineering. J Controlled Release 2003;87(1):69–79.
12. Oh S-Y, Kang M-S, Knowles JC, Gong MS. Synthesis of biobased thermoplastic polyurethane elastomers containing isosorbide and polycarbonate diol and their biocompatible properties. J Biomater Appl 2015;30(3):327–337.
13. Wang S, Yaszemski MJ, Gruetzmacher JA, Lu L. Photo-crosslinked poly(ε-caprolactone fumarate) networks: Roles of crystallinity and crosslinking density in determining mechanical properties. Polymer 2008;49(26):5692–5699.
14. Wu Y, Shi X, Li Y, Tian L, Bai R, Wei Y, Han D, Liu H, Xu J. Carbon nanohorns promote maturation of neonatal rat ventricular myocytes and inhibit proliferation of cardiac fibroblasts: A promising scaffold for cardiac tissue engineering. Nanoscale Res Lett 2016;11(1):1–9.
15. Peña B, Martinelli V, Jeong M, Bosi S, Lapasin R, Taylor MRG, Long CS, Shandas R, Park D, Mestroni L. Biomimetic polymers for cardiac tissue engineering. Biomacromolecules 2016;17(5): 1593–1601.
16. Wang S, Lu L, Gruetzmacher J, Currier B, Yaszemski M. Synthesis and characterizations of biodegradable and crosslinkable poly(ε-caprolactone fumarate), poly(ethylene glycol fumarate), and their amphiphilic copolymer. Biomaterials 2006;27(6):832–841.

17. Basu P, Repanas A, Chatterjee A, Glasmacher B, Narendra Kumar U, Manjubala I. PEO–CMC blend nanofibers fabrication by electrospinning for soft tissue engineering applications. Mater Lett 2017; 195:10–13.
18. Ji C, Shi J, Thermal-crosslinked porous chitosan scaffolds for soft tissue engineering applications. Mater Sci Eng C 2013;33(7):3780–3785.
19. Kakkar P, Verma S, Manjubala I, Madhan B. Development of keratin–chitosan–gelatin composite scaffold for soft tissue engineering. Mater Sci Eng C 2014;45:343–347.
20. Jallerat Q, Szymanski JM, Feinberg AW, Nano-and microstructured ECM and biomimetic scaffolds for cardiac tissue engineering. In: Bio-Inspired Material for Biomedical Engineering. New York: Wiley; 2014.
21. Oh B, Lee CH. Nanofiber for cardiovascular tissue engineering. Expert Opin Drug Deliv 2013;10(11):1565–1582.
22. Sant S, Khademhosseini A. Fabrication and characterization of tough elastomeric fibrous scaffolds for tissue engineering applications. In: 2010 Annual International Conference of the IEEE Engineering in Medicine and Biology. IEEE; 2010.
23. Díaz-Herráez P, Garbayo E, Simón-Yarza T, Formiga FR, Prosper F, Blanco-Prieto MJ. Adipose-derived stem cells combined with neuregulin-1 delivery systems for heart tissue engineering. Eur J Pharm Biopharm 2013;85(1):143–150.
24. Tian S, Ma PX, Wang Z, Liu Q, Gnatovskiy L. Heart regeneration with embryonic cardiac progenitor cells and cardiac tissue engineering. J Stem Cell Transplant. Biol 2015;1(1):104.
25. Bittiger H, Marchessault R, Niegisch W. Crystal structure of poly-ε-caprolactone. Acta Crystallogr Sect B 1970;26(12):1923–1927.
26. Wang X, Zhao H, Turng L-S, Li Q. Crystalline morphology of electrospun poly (ε-caprolactone)(PCL) nanofibers. Ind Eng Chem Res 2013;52(13):4939–4949.
27. Runge MB, Wang H, Spinner RJ, Windebank AJ, Yaszemski MJ. Reformulating polycaprolactone fumarate to eliminate toxic diethylene glycol: Effects of polymeric branching and autoclave sterilization on material properties. Acta Biomater 2012;8(1):133–143.
28. Wang S, Yaszemski MJ, Knight AM, Gruetzmacher JA, Windebank AJ, Lu L. Photo-crosslinked poly (ε-caprolactone fumarate) networks for guided peripheral nerve regeneration: Material properties and preliminary biological evaluations. Acta Biomater 2009;5(5):1531–1542.
29. Martins AM, Eng G, Caridade SG, Mano JF, Reis RL, Vunjak-Novakovic G. Electrically conductive chitosan/carbon scaffolds for cardiac tissue engineering. Biomacromolecules 2014;15(2):635–643.
30. Sharifi S, Mirzadeh H, Imani M, Atai M, Ziaee F. Photopolymerization and shrinkage kinetics of in situ crosslinkable N-vinyl-pyrrolidone/poly (ε-caprolactone fumarate) networks. J Biomed Mater Res Part A 2008;84(2):545–556.
31. Yu J, Lee A-R, Lin W-H, Lin C-W, Wu Y-K, Tsai W-B. Electrospun PLGA fibers incorporated with functionalized biomolecules for cardiac tissue engineering. Tissue Eng Part A 2014;20(13–14): 1896–1907.
32. Brett Runge M, Dadsetan M, Baltrusaitis J, Knight AM, Ruesink T, Lazcano EA, Lu L, Windebank AJ, Yaszemski MJ. The development of electrically conductive polycaprolactone fumarate–polypyrrole composite materials for nerve regeneration. Biomaterials 2010;31(23):5916–5926.
33. Sharifi S, Shafieyan Y, Mirzadeh H, Bagheri-Khoulenjani S, Rabiee SM, Imani M, Atai M, Shokrgozar MA, Hatampoor A. Hydroxyapatite scaffolds infiltrated with thermally crosslinked polycaprolactone fumarate and polycaprolactone itaconate. J Biomed Mater Res Part A 2011;98(2):257–267.
34. Farokhi M, Sharifi S, Shafieyan Y, Bagher Z, Mottaghitalab F, Hatampoor A, Imani M, Shokrgozar MA. Porous crosslinked poly (ε-caprolactone fumarate)/nanohydroxyapatite composites for bone tissue engineering. J Biomed Mater Res Part A 2012;100(4): 1051–1060.
35. Lin W-H, Tsai W-B. In situ UV-crosslinking gelatin electrospun fibers for tissue engineering applications. Biofabrication 2013;5(3): 035008.
36. Zeytuncu B, Akman S, Yucel O, Kahraman MV. Synthesis and adsorption application of in situ photo-cross-linked electrospun poly (vinyl alcohol)-based nanofiber membranes. Water Air Soil Pollution 2015;226(6):1–20.
37. Wu R, Zhang J-F, Fan Y, Stoute D, Lallier T, Xu X. Reactive electrospinning and biodegradation of cross-linked methacrylated polycarbonate nanofibers. Biomed Mater 2011;6(3):035004.
38. Wang H, Feng Y, An B, Zhang W, Sun M, Fang Z, Yuan W, Khan M. Fabrication of PU/PEGMA crosslinked hybrid scaffolds by in situ UV photopolymerization favoring human endothelial cells growth for vascular tissue engineering. J Mater Sci Mater Med 2012;23(6):1499–1510.
39. Mirmohammadi SA, Imani M, Uyama H, Atai M. In situ photo-crosslinkable nanohybrids based on poly (ε-caprolactone fumarate)/polyhedral oligomeric silsesquioxane: Synthesis and characterization. J Polym Res 2013;20(12):1–13.
40. Kenar H, Kose GT, Toner M, Kaplan DL, Hasirci V. A 3D aligned microfibrous myocardial tissue construct cultured under transient perfusion. Biomaterials 2011;32(23):5320–5329.
41. Pok S, Myers JD, Madihally SV, Jacot JG. A multilayered scaffold of a chitosan and gelatin hydrogel supported by a PCL core for cardiac tissue engineering. Acta Biomater 2013;9(3):5630–5642.